Journal of Power Sources 196 (2011) 10126–10132

Contents lists available at ScienceDirect

Journal of Power Sources

journal homepage: www.elsevier.com/locate/jpowsour

Effects of supersonic treatment on the electrochemical properties and crystal structure of $LiMn_{1.5}Ni_{0.5}O_4$ as a cathode material for Li ion batteries

Hidesato Saruwatari[a,b], Tadaomi Ishikawa[a], Yoshiyuki Korechika[a], Naoto Kitamura[a], Norio Takami[c], Yasushi Idemoto[a,*]

[a] Department of Pure and Applied Chemistry, Faculty of Science and Technology, Tokyo University of Science, 2641 Yamazaki, Noda, Chiba 278-8510, Japan
[b] Saku Operations, Transmission Distribution and Industrial Systems Company Toshiba Corporation, 9, Nenei, Saku, Nagano 385-0012, Japan
[c] Functional Materials Laboratory, Corporate Research and Development Center, Toshiba Corporation, 1, Komukai-Toshiba-cho, Saiwai-ku, Kawasaki 212-8582, Japan

ARTICLE INFO

Article history:
Received 6 April 2011
Received in revised form 7 July 2011
Accepted 4 August 2011
Available online 10 August 2011

Keywords:
Li ion battery
Cathode material
$LiMn_{1.5}Ni_{0.5}O_4$
Supersonic-wave
Crystal structure

ABSTRACT

The electrochemical properties and crystal structure of $LiMn_{1.5}Ni_{0.5}O_4$ treated with supersonic waves in an aqueous Ni-containing solution were investigated by performing charge–discharge tests, inductively coupled plasma (ICP) analysis, scanning electron microscopy (SEM), iodometry, X-ray diffraction (XRD), powder neutron diffraction and synchrotron powder XRD. The charge–discharge curve of $LiMn_{1.5}Ni_{0.5}O_4$ versus Li/Li^+ has plateaus at 4.1 and 4.7 V. The 4.1 V versus Li/Li^+ plateau due to the oxidation of $Mn^{3+/4+}$ was reduced by the supersonic treatment. During the charge–discharge cycling test at 25 °C, the supersonic treatment increased the discharge capacity of the 50th cycle. Rietveld analysis of the neutron diffraction patterns revealed that the Ni occupancy of the 4b site in $LiMn_{1.5}Mn_{0.5}O_4$, which is mainly occupied by Ni, was increased by the supersonic treatment. This result suggests that Ni^{2+} is partially substituted for $Mn^{3+/4+}$ during the supersonic treatment.

1. Introduction

There has been increasing interest in finding suitable high-voltage cathode materials in the 5 V region for lithium ion batteries due to their high power densities. Lithium manganese oxide with a spinel structure has a 4.7–4.9 V plateau when 3d-transition metals are substituted for Mn to form $LiMn_{2-x}M_xO_4$ (M = Co, Cr, Cu, Fe, Ni) [1–3]. Of these materials, $LiMn_{1.5}Ni_{0.5}O_4$ is a promising next-generation cathode material for lithium-ion batteries for electric vehicles (EVs) and plug-in hybrid electric vehicles (PHEVs) due to its excellent rate capability and good cycling ability [2,3]. However, its cathode performance in the 4 V region, charge–discharge behavior, and cycle performance vary depending on the method used to synthesize it [2–4]. $LiMn_{1.5}Ni_{0.5}O_4$ synthesized by the solid-state method has a Ni solubility limit of 0.430 [2]. Various methods for synthesizing $LiMn_{1.5}Ni_{0.5}O_4$ have been reported [2–10]. It decomposes the electrolyte due to its high discharge potential, but coating the cathode material with an inorganic film suppresses the electrolyte decomposition [11]. Therefore, the partial substitution and/or surface coating are effective for enhancing the $LiMn_{1.5}Ni_{0.5}O_4$ performance.

We have recently investigated using supersonic treatment a partial substitution and surface coating method. We found that the cathode performance of $LiMnO_4$ was improved by supersonic treatment in a Zn-containing aqueous solution [12,13]. In the present study, we investigated the improvement in the electrochemical properties and the change in the crystal structure of $LiMn_{1.5}Ni_{0.5}O_4$ upon supersonic treatment in an aqueous Ni-containing solution. We performed supersonic treatment on $LiMn_{1.5}Ni_{0.5}O_4$ powder that had been synthesized by a solid-state method in an aqueous Ni-containing solution. The obtained powder was characterized by X-ray diffraction (XRD), chemical composition and Mn valence analysis. In addition, its electrochemical properties were investigated. We also performed a Rietveld analysis (RIETAN-FP [14]) of the neutron diffraction patterns and investigated the electron density distribution by the maximum entropy method (MEM: PRIMA [15]) of synchrotron powder XRD patterns. Based on these results, we discuss the effect of the supersonic treatment on the $LiMn_{1.5}Ni_{0.5}O_4$ powder.

2. Experimental

$LiMn_{1.5}Ni_{0.5}O_4$ was synthesized by a solid-state reaction using Li_2CO_3, MnO_2 and $Ni(OH)_2$ as the starting materials. The mixture was preheated at 600 °C for 24 h in air and then heat-treated at 700 °C for 24 h in O_2. Supersonic treatment consisted of a first step at a frequency of 28 kHz and a second step at a fre-

* Corresponding author. Tel.: +81 4 7122 9493; fax: +81 4 7125 7761.
E-mail address: idemoto@rs.noda.tus.ac.jp (Y. Idemoto).

0378-7753/$ – see front matter © 2011 Elsevier B.V. All rights reserved.
doi:10.1016/j.jpowsour.2011.08.016

Table 1
Experimental conditions and lattice constants of the samples with the supersonic-wave treatments. That of untreated $LiMn_{1.5}Ni_{0.5}O_4$ is also listed as a reference.

Sample	Frequency (kHz)	Ni concentration (wt%)	Treatment time (min)	a (nm)
(A)	–	–	–	0.8159(1)
(B)	28	1.0	40	0.8162(1)
(C)	28	1.0	60	0.8158(1)
(D)	28	1.0	90	0.8168(1)
(E)	28	1.0	10×6	0.8149(2)
(F)	$28 \rightarrow 200$	1.0	$20 \rightarrow 20$	0.8155(1)
(G)	28	4.0	40	0.81708(8)
(H)	28	4.0	60	0.8174(1)

quency of 200 kHz with a power of 300 W. It was applied to the obtained $LiMn_{1.5}Ni_{0.5}O_4$ powder in an aqueous Ni-containing solution, which was prepared by dissolving nickel acetate (99.9%, Wako Pure Chemical Industries, Ltd.) in distilled water. The weight ratios of the nickel acetate to distilled water were 4:96 and 1:99. The supersonic treatment was performed at room temperature for 40–90 min. After the supersonic treatment, $LiMn_{1.5}Ni_{0.5}O_4$ powder was heated at 600 °C for 2 h in air. Table 1 summarizes the experimental conditions for the eight produced samples. The obtained samples were examined by powder XRD (Philips, X'Pert Pro) and their metal composition was determined by inductively coupled plasma (ICP) analysis (Shimadzu Co., ICPS-7500). The Mn valance was determined by chemical analysis. The powder morphologies were observed by scanning electron microscopy (SEM) (Hitachi, S-2600N). We performed a Rietveld analysis (RIETAN-FP) of the powder neutron diffraction data (HERMES, JRR-3) and synchrotron powder XRD data (BL19B2, SPring-8). To determine the electronic structure, we investigated the electron density distribution by applying the MEM to the synchrotron powder XRD data (BL19B2, SPring-8).

The electrochemical properties of the samples after the supersonic treatment were investigated. A conventional three-electrode cell was used. The working electrodes were prepared by mixing the active material, acetylene black, graphite and polyvinylidene difluoride (PVdF) in the weight ratio of 100:2.5:2.5:3.5. Li metal foils were utilized as the counter and reference electrodes. One molar $LiPF_6$, in a mixed solvent of ethylene carbonate (EC) and dimethyl carbonate (DMC) with 50:50 vol.% (Li-battery grade, Tomiyama Pure Chemical Industries, Ltd.) was used as the electrolyte. A glass filter was used as the separator. The charge and discharge performance was measured using a potentio-galvanostat (Solartron, SI1287). The cell was first charged to 5.0 V versus Li/Li^+ at 27 mA g^{-1} (charge condition 1) or a 4.9 V versus the Li/Li^+ constant-current–constant-voltage (CC–CV) mode for 10 h at 27 mA g^{-1} (charge condition 2) or 5.0 V versus the Li/Li^+ CC–CV mode for 10 h at 27 mA g^{-1} (charge condition 3). The cell was then discharged to 3.5 V versus Li/Li^+ at 27 mA g^{-1}. The charge–discharge cycling performance was investigated by repeating the charging and discharging process 50 times at a constant current of 135 mA g^{-1} at 25 °C. The limiting discharge voltage was 3.5 V versus Li/Li^+, and the charging condition was fixed at a current of 135 mA g^{-1} to 4.9 V versus Li/Li^+ followed by a constant voltage until the charging current of 6.75 mA g^{-1} was achieved.

3. Results and discussion

3.1. Sample characterization

Fig. 1 shows the powder XRD patterns of samples that had been subjected to the supersonic treatment. The XRD pattern of $LiMn_{1.5}Ni_{0.5}O_4$ that had not been subjected to the supersonic treatment is also given as a reference. All the diffraction peaks of the samples could be assigned to the spinel structure (space group: Fd-3m), indicating that only a single phase was obtained. Table 1 lists

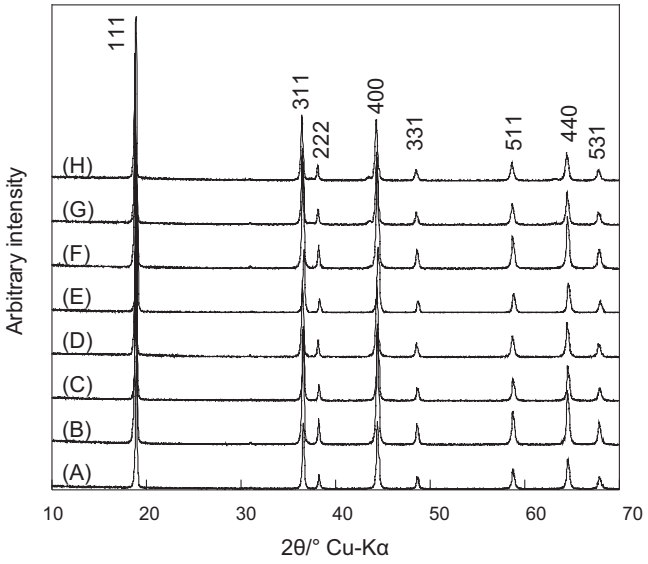

Fig. 1. X-ray diffraction patterns of $LiMn_{1.5}Ni_{0.5}O_4$ and the sample after the supersonic-wave treatment and the subsequent heat-treatment. (A) Untreated, (B) 28 kHz, 1.0 wt% Ni, 40 min, (C) 28 kHz, 1.0 wt% Ni, 60 min, (D) 28 kHz, 1.0 wt% Ni, 90 min, (E) 28 kHz, 1.0 wt% Ni, 10×6 min, (F) $28 \rightarrow 200$ kHz, 1.0 wt% Ni, $20 \rightarrow 20$ min, (G) 28 kHz, 4.0 wt% Ni, 40 min, (H) 28 kHz, 4.0 wt% Ni, 60 min.

the lattice constants calculated from the XRD patterns. The samples that had been subjected to the supersonic treatment had similar lattice constants as the sample that had not been supersonically treated. Table 2 shows the composition ratios of the metallic element and the Mn/Ni ratio determined by an ICP analysis. The Mn/Ni ratio approached three after the supersonic treatment. Table 3 shows the transition metal valences and the oxygen contents of

Table 2
Compositions of samples with supersonic-wave treatments in Ni aqueous solution. That of untreated $LiMn_{1.5}Ni_{0.5}O_4$ is also listed as a reference.

Sample	Li	Mn	Ni	Mn/Ni
(A) Untreated	1.000(1)	1.536(2)	0.462(1)	3.31
(B) 28 kHz, 1.0 wt% Ni, 40 min	0.990(2)	1.524(2)	0.487(2)	3.13
(C) 28 kHz, 1.0 wt% Ni, 60 min	0.987(3)	1.527(1)	0.485(2)	3.15
(D) 28 kHz, 1.0 wt% Ni, 90 min	0.948(2)	1.5592(9)	0.492(1)	3.17
(E) 28 kHz, 1.0 wt% Ni, 10×6 min	0.958(5)	1.552(5)	0.4895(6)	3.17
(F) $28 \rightarrow 200$ kHz, 1.0 wt% Ni, $20 \rightarrow 20$ min	1.003(2)	1.509(3)	0.488(1)	3.09
(G) 28 kHz, 4.0 wt% Ni, 40 min	0.934(2)	1.510(1)	0.554(1)	2.72
(H) 28 kHz, 4.0 wt% Ni, 60 min	1.000(2)	1.481(6)	0.519(2)	2.85

Table 3
Average valence of Mn and Ni, and oxygen content of sample (A), (B) and (C).

Sample	Transition metal valence	Amount of oxygen
(A) Untreated	3.42(2)	3.92
(B) 28 kHz, 1.0 wt% Ni, 40 min	3.46(2)	3.97
(C) 28 kHz, 1.0 wt% Ni, 60 min	3.49(1)	3.99

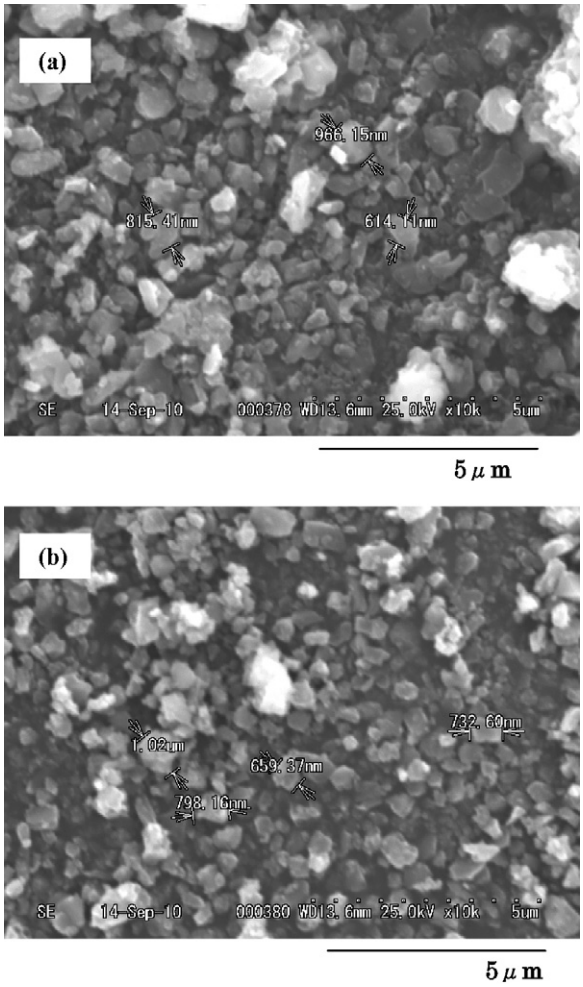

Fig. 2. SEM images of (a) $LiMn_{1.5}Ni_{0.5}O_4$ [sample (A)] and (b) samples after the supersonic-wave treatments in 1.0 wt% Ni aqueous solution [sample (B)].

Table 4
Aqueous solution concentration after supersonic-wave treatment.

Sample	Li (ppm)	Mn (ppm)	Ni (ppm)
Blank	0.367(3)	0.0398(5)	11.7(1)
(B) 28 kHz, 1.0 wt% Ni, 40 min	0.263(2)	0.0024(1)	5.36(3)
(C) 28 kHz, 1.0 wt% Ni, 60 min	0.366(2)	0.0067(0)	6.72(6)
(F) 28 → 200 kHz, 1.0 wt% Ni, 20 + 20 min	0.315(4)	0.0109(1)	6.22(7)

samples A, B, and C determined by iodometry and ICP analyses. Supersonic treatment in the aqueous Ni solution increased the transition metal valence. These results suggested that Ni^{2+} is partially substituted for $Mn^{3+/4+}$ during the supersonic treatment and heat treatment. Fig. 2 shows SEM images of samples A and B. They reveal that the particle size did not change during the supersonic treatment. Table 4 shows the aqueous solution concentrations after the supersonic treatment of samples B, C, and F determined by ICP analysis. The data for a 1 wt% Ni aqueous solution that had been stored with untreated $LiMn_{1.5}N_{i0.5}O_4$ for 10 min at room temperature is also shown for comparison. The supersonic treatment did not change the Li and Mn concentrations, indicating that Li and Mn had not dissolved in the aqueous Ni solution. In contrast, supersonic treatment reduced the Ni concentration. These results are consistent with the ICP and iodometry data.

Table 5
Charge and discharge capacities at 1st cycle, and the coulomb efficiency (%) of the samples with supersonic-wave treatments in Ni aqueous solution. That of untreated $LiMn_{1.5}Ni_{0.5}O_4$ is also listed as a reference.

Sample	Charge capacity (mAh/g)	Discharge capacity (mAh/g)	Coulomb efficiency (%)
(A) Untreated	159.7	135.9	85.1
(B) 28 kHz, 1.0 wt% Ni, 40 min	159.1	136.6	85.9
(C) 28 kHz, 1.0 wt% Ni, 60 min	159.7	137.1	85.9
(D) 28 kHz, 1.0 wt% Ni, 90 min	159.6	136.0	85.2
(E) 28 kHz, 1.0 wt% Ni, 10 × 6 min	159.4	135.3	84.9
(F) 28 → 200 kHz, 1.0 wt% Ni, 20 → 20 min	154.8	139.3	90.3
(G) 28 kHz, 4.0 wt% Ni, 40 min	145.6	130.4	89.6
(H) 28 kHz, 4.0 wt% Ni, 60 min	145.5	131.7	90.5

Charge: 27 mA g^{-1} (0.2 C rate) to 4.9 V versus Li/Li^+ followed by a constant voltage of 4.9 V versus Li/Li^+ for a total of 10 h (charge condition 2); discharge: 27 mA g^{-1} (0.2 C rate) to 3.5 V versus Li/Li^+.

Table 6
Charge and discharge capacities at 1st cycle, and the coulomb efficiency (%) of the sample (A) and (B).

		(A) Untreated	(B) 28 kHz, 1.0 wt% Ni 40 min
Charge condition 1	Charge capacity (mAh/g)	145.4	149.7
	Discharge capacity (mAh/g)	136.9	137.1
	Coulomb efficiency (%)	94.2	91.6
Charge condition 2	Charge capacity (mAh/g)	159.7	159.1
	Discharge capacity (mAh/g)	135.9	136.6
	Coulomb efficiency (%)	85.1	85.9
Charge condition 3	Charge capacity (mAh/g)	184.1	172.5
	Discharge capacity (mAh/g)	132.7	136.1
	Coulomb efficiency (%)	72.1	78.9

Charge condition 1: 27 mA g^{-1} (0.2 C rate) to 5.0 V versus Li/Li^+; charge condition 2: 27 mA g^{-1} (0.2 C rate) to 4.9 V versus Li/Li^+ followed by a constant voltage of 4.9 V versus Li/Li^+ for a total of 10 h; Charge condition 3: 27 mA g^{-1} (0.2 C rate) to 5.0 V versus Li/Li^+ followed by a constant voltage of 4.9 V versus Li/Li^+ for a total of 10 h; discharge: 27 mA g^{-1} (0.2 C rate) to 3.5 V versus Li/Li^+.

3.2. Electrochemical property

Fig. 3 shows the first charge–discharge curves of the samples at 25 °C. The cell was operated under charge conditions 2 (Fig. 3(a)), 1(Fig. 3(c)) and 3 (Fig. 3(d)). The cell was then discharged to 3.5 V versus Li/Li^+ at 27 mA g^{-1}. Tables 5 and 6 list the first charge and discharge capacities and coulomb efficiencies. The 4.1 V versus Li/Li^+ plateau due to the oxidation of $Mn^{3+/4+}$ was reduced by the supersonic treatment. These results are consistent with the ICP and iodometry data. The discharge capacity of the sample that had been subjected to the supersonic treatment in a 1 wt% Ni aqueous solution increased, whereas the discharge capacity of the sample that had been subjected to supersonic treatment in the 4 wt% Ni aqueous solution decreased. This indicated that the increase in the discharge capacity upon supersonic treatment in the 1 wt% Ni aque-

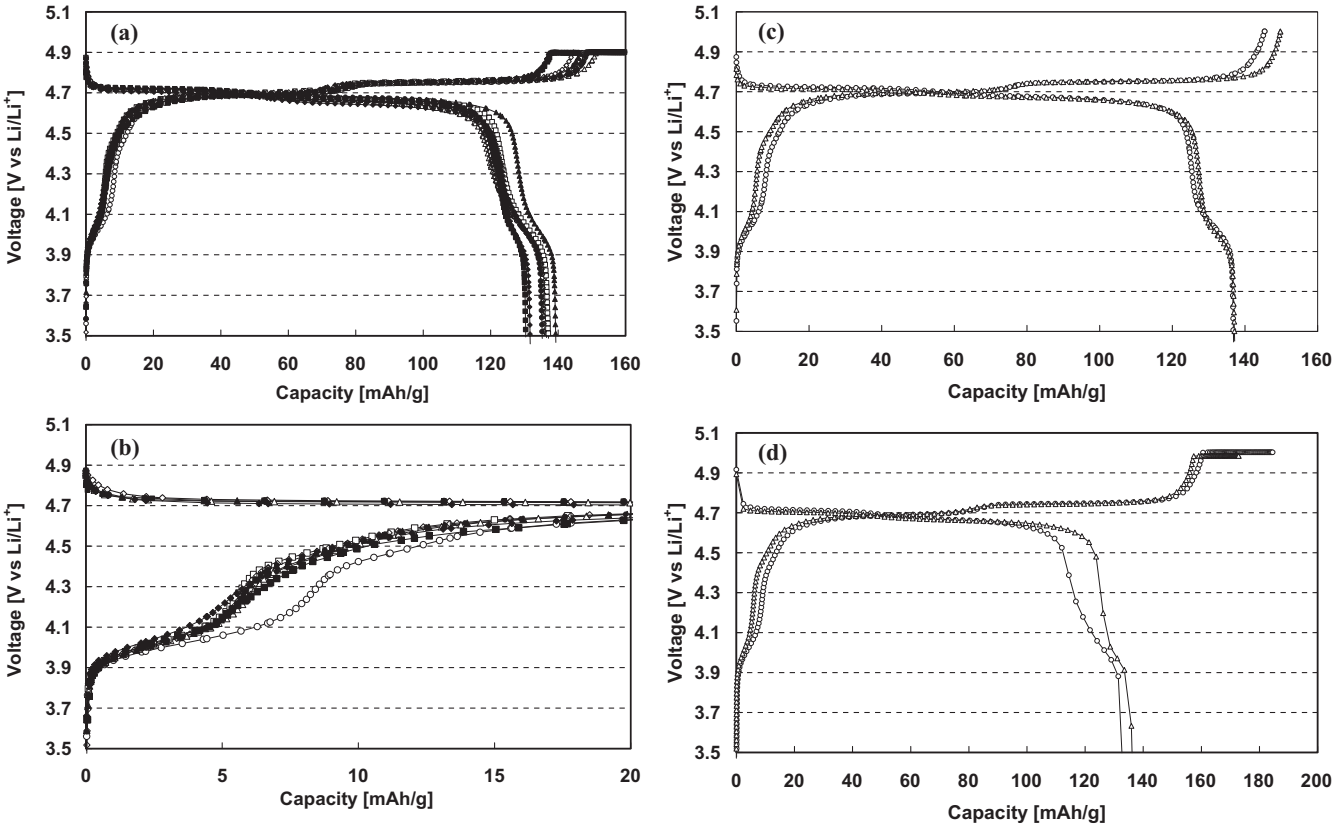

Fig. 3. Charge and discharge curves at the first cycle at room temperature. (a) Charge: 27 mA g^{-1} (0.2 C rate) to 4.9 V versus Li/Li^+ followed by a constant voltage of 4.9 V versus Li/Li+ for a total of 10 h (charge condition 2). (b) Enlargement of (a) and (c) charge: 27 mA g^{-1} (0.2 C rate) to 5.0 V versus Li/Li^+ (charge condition 1). (d) Charge: 27 mA g^{-1} (0.2 C rate) to 5.0 V versus Li/Li^+ followed by a constant voltage of 4.9 V versus Li/Li^+ for a total of 10 h (charge condition 3). Discharge: 27 mA g^{-1} (0.2 C rate) to 3.5 V versus Li/Li^+. ○: (A) untreated, △: (B) 28 kHz, 1.0 wt% Ni, 40 min, □: (C) 28 kHz, 1.0 wt% Ni, 60 min, ◊: (D) 28 kHz, 1.0 wt% Ni, 90 min, ●: (E) 28 kHz, 1.0 wt% Ni, 10 × 60 min, ▲: (F) 28 → 200 kHz, 1.0 wt% Ni, 20 → 20 min, ■: (G) 28 kHz, 4.0 wt% Ni, 40 min, ♦: (H) 28 kHz, 4.0 wt% Ni, 60 min.

ous solution is due to partial substitution of Ni^{2+} for $Mn^{3+/4+}$. On the other hand, the Ni content, which does not contribute to the charging and discharging, increased upon supersonic treatment in the 4 wt% Ni aqueous solution. Using samples A and B, we compared the coulomb efficiency of the first cycle for the different first charging conditions. For charge condition 1, sample A has a higher coulomb efficiency than sample B, whereas the coulomb efficiency of sample A was almost equal to that of sample B for charge condition 2. On the other hand, sample A has a lower coulomb efficiency than sample

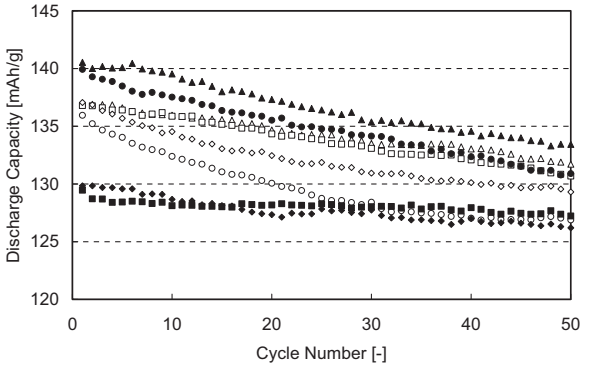

Fig. 4. Cycle performances at room temperature for $LiMn_{1.5}Ni_{0.5}O_4$ and the sample after the supersonic-wave treatment and the subsequent heat-treatment. ○: (A) untreated, △: (B) 28 kHz, 1.0 wt% Ni, 40 min, □: (C) 28 kHz, 1.0 wt% Ni, 60 min, ◊: (D) 28 kHz, 1.0 wt% Ni, 90 min, ●: (E) 28 kHz, 1.0 wt% Ni, 10 × 6 min, ▲: (F) 28 → 200 kHz, 1.0 wt% Ni, 20 → 20 min, ■: (G) 28 kHz, 4.0 wt% Ni, 40 min, ♦: (H) 28 kHz, 4.0 wt% Ni, 60 min.

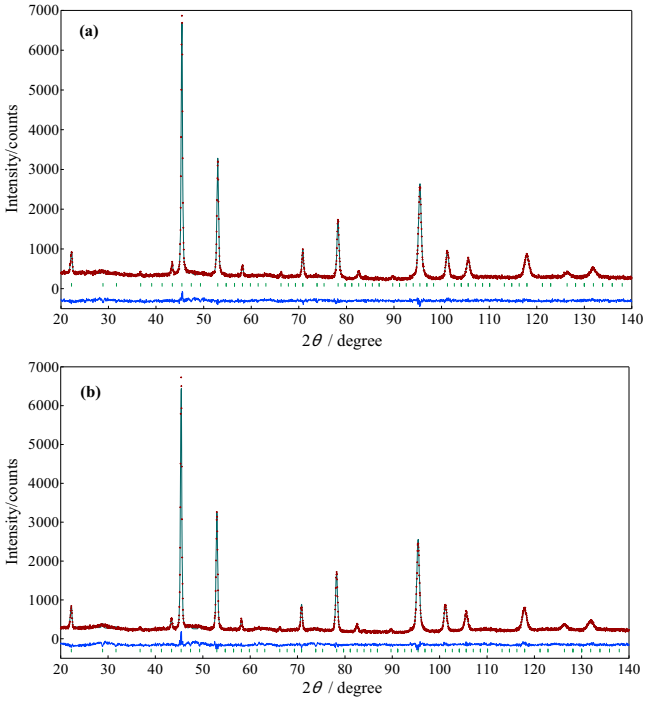

Fig. 5. Rietveld refinement pattern. Plus marks show observed intensities, and a solid line represents calculated intensities. Vertical marks below them indicate positions of allowed Bragg refractions. A curve at the bottom is a difference between the observed and calculated intensities in the same scale. (a) Sample (A) untreated, (b) Sample (B) 28 kHz, 1.0 wt% Ni, 40 min.

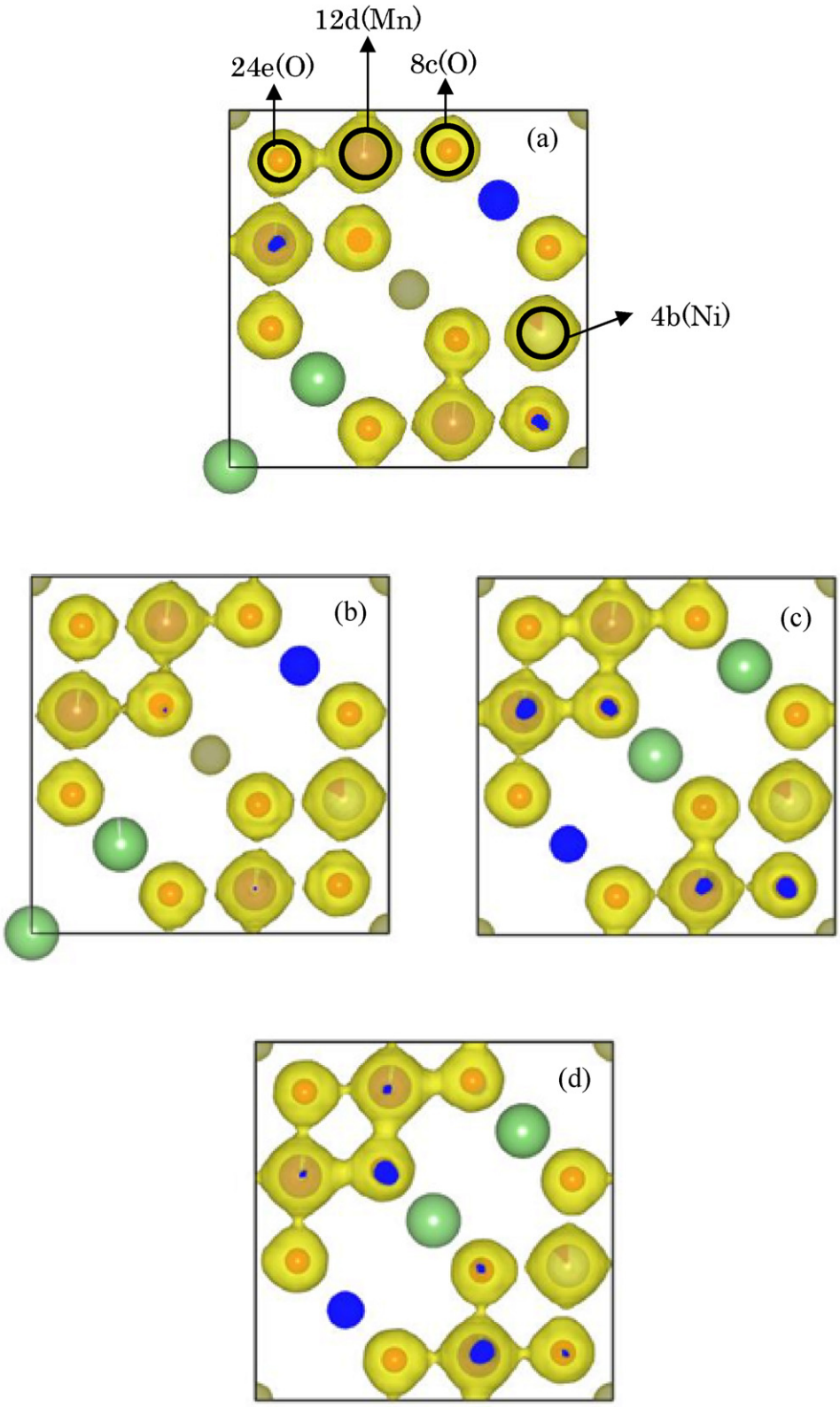

Fig. 6. Electron density image in (110) plane by MEM (Maximum Entropy Method). (a) Sample (A) untreated, (b) Sample (B) 28 kHz, 1.0 wt% Ni, 40 min, (c) Sample (C) 28 kHz, 1.0 wt% Ni, 60 min, (d) Sample (F) 28 → 200 kHz, 1.0 wt% Ni, 20 → 20 min.

B for charge condition 3. These results suggest that the supersonic treatment suppresses the electrolyte decomposition at high voltages.

Fig. 4 shows plots of the discharge capacities as a function of the cycle number. Table 7 lists the second and 50th discharge capacities and capacity retentions. The cycle performance was improved by the supersonic treatment, especially that of sample B. These results suggest that the supersonic treatment suppresses the partial substitution of $Mn^{3+/4+}$ for Ni^{2+} and electrolyte decomposition at high voltages.

Table 7
Discharge capacities at 2nd and 50th cycles, and the capacity retentions (%) of untreated $LiMn_{1.5}Ni_{0.5}O_4$ and the samples with the supersonic-wave treatments.

Sample	Capacity at 2nd cycle (mAh/g)	Capacity at 50th cycle (mAh/g)	Capacity retention (%)
(A) Untreated	135.9	126.9	93.4
(B) 28 kHz, 1.0 wt% Ni, 40 min	137.0	131.7	96.1
(C) 28 kHz, 1.0 wt% Ni, 60 min	136.8	130.7	95.5
(D) 28 kHz, 1.0 wt% Ni, 90 min	137.1	129.3	94.3
(E) 28 kHz, 1.0 wt% Ni, 10 × 6 min	139.9	130.9	93.6
(F) 28 → 200 kHz, 1.0 wt% Ni, 20 → 20 min	140.5	133.4	94.9
(G) 28 kHz, 4.0 wt% Ni, 40 min	129.5	127.2	98.2
(H) 28 kHz, 4.0 wt% Ni, 60 min	129.8	126.2	97.2

Table 8
Final results of Rietveld refinements for Sample (A) and (B) in space group $P4_332$ at room temperature.

(a)

Atom	Site	x	y	z	$10^2 \times B$ (nm^2)	Site occupancy
Li1	8c	1.003(3)	=Li(x)	=Li(x)	0.6(2)	1
Ni1	4b	=Mn1(x)	=Mn1(y)	=Mn1(z)	=Mn1(B)	0.431(4)
Mn1	4b	3/8	3/8	3/8	3	0.565(4)
Mn2	12d	1/8	0.384(2)	1/4-y	1.1(4)	0.836(4)
Ni2	12d	=Mn2(x)	=Mn2(y)	=Mn2(z)	=Mn2(B)	0.164(4)
O1	8c	0.3890(7)	=O1(x)	=O1(x)	0.1	1
O2	24e	0.1100(8)	0.1138(6)	0.3867(6)	0.98(6)	1

(b)

Atom	Site	x	y	z	$10^2 \times B$ (nm^2)	Site occupancy
Li1	8c	1.002(3)	=Li(x)	=Li(x)	1.0(2)	0.99
Ni1	4b	=Mn1(x)	=Mn1(y)	=Mn1(z)	=Mn1(B)	0.470(4)
Mn1	4b	3/8	3/8	3/8	3	0.552(4)
Mn2	12d	1/8	0.384(2)	$1/4 - y$	0.6(4)	0.832(4)
Ni2	12d	=Mn2(x)	=Mn2(y)	=Mn2(z)	=Mn2(B)	0.168(4)
O1	8c	0.3880(7)	=O1(x)	=O1(x)	0.1	1
O2	24e	0.1097(8)	0.1148(6)	0.3877(6)	1.06(7)	0.99(1)

(a) Sample (A): a = 0.81573(3) nm, R_{wp} = 5.98%, R_p = 4.66%, R_{exp} = 4.96%, S = 1.21; (b) Sample (B): a = 0.81627(3) nm, R_{wp} = 7.71%, R_p = 5.91%, R_{exp} = 5.57%, S = 1.39.

3.3. Crystal structure analysis

To investigate why the electrochemical properties of $LiMn_{1.5}Ni_{0.5}O_4$ were improved by the supersonic treatment, powder neutron diffraction measurements were performed and the crystal structure was determined by a Rietveld analysis. Fig. 5 shows the Rietveld refinement patterns for samples A and B calculated from the powder neutron diffraction pattern. Table 8 lists the refined structure parameters and the R values. The Rietveld refinement results show good agreement with the experimental data. The values of R_{wp} and S are sufficiently low. The lattice constants slightly increased due to the supersonic treatment. This increase in the lattice constants suggests that the supersonic treatment in a Ni-containing aqueous solution causes the partial substitution of Ni^{2+} for $Mn^{3+/4+}$. The supersonic treatment increased the Ni occupancy of the 4b site. The analytical results indicated that supersonic treatment in an aqueous Ni-containing solution eliminated the Ni deficiency of the 4b site for $LMn_{1.5}Ni_{0.5}O_4$ synthesized by the solid-state method. These results are consistent with the ICP, iodometry and electrochemical properties data.

We also obtained synchrotron XRD patterns and then estimated the electron density from the experimental data using the MEM. Fig. 6 shows the electron density distribution map in the (1 1 0) plane obtained by applying the MEM to the synchrotron XRD patterns for samples A, B, C, and F. For all the samples, the electron density between 4b-O was lower than that between 12d-O. The 4b site is mainly occupied by Ni, whereas the 12d site is mainly occupied by Mn. This indicates that the Mn–O covalent bond affects the structural stability of the $LiMn_{1.5}Ni_{0.5}$ O_4. $LiMn_{1.5}Ni_{0.5}O_4$ that had not been subjected to the supersonic treatment has a higher electron density between 12d and 24e than the sample that had been subjected to the supersonic treatment. On the other hand, $LiMn_{1.5}Ni_{0.5}O_4$ that had been subjected to the supersonic treatment had a higher electron density between 12d and 8c than that of the sample that not been subjected to the supersonic treatments. These results suggest that the good cycling performance originates from the 12d to 8c bond strength.

4. Conclusion

The electrochemical properties of $LiMn_{1.5}Ni_{0.5}O_4$ were improved by supersonic treatment in an aqueous Ni-containing solution. ICP and iodometry data revealed that the supersonic treatment increased the transition metal valence of $LiMn_{1.5}Ni_{0.5}O_4$. These analyses suggest that Ni^{2+} is partially substituted for $Mn^{3+/4+}$. Supersonic treatment reduced the 4.1 V versus Li/Li^+ plateau in the first charge curve due to oxidation of $Mn^{3+/4+}$. The supersonic treatment also improved the cycle performance of the $LiMn_{1.5}Ni_{0.5}O_4$.

The crystal structures of $LiMn_{1.5}Ni_{0.5}O_4$ obtained from the neutron diffraction patterns revealed that the Ni occupancy of the 4b site, which was mainly occupied by Ni in the $LiMn_{1.5}Ni_{0.5}O_4$, is increased by the supersonic-wave treatments. The improvement in the cycling performance of $LiMn_{1.5}Ni_{0.5}O_4$ upon supersonic treatment is thought to be due to the partial substitution of Ni^{2+} for $Mn^{3+/4+}$.

References

[1] C. Sigala, D. Guyomard, A. Verbaere, Y. Piffard, M. Tournoux, Solid State Ionics 81 (1995) 167.
[2] Q. Zhong, A. Bonakdarpour, M. Zhang, Y. Gao, J.R. Dahn, J. Electrochem. Soc. 144 (1997) 205.

[3] T. Ohzuku, S. Takeda, M. Iwanaga, J. Power Sources 81–82 (1999) 90.
[4] Y. Idemoto, H. Narai, N. Koura, J. Power Sources 191–121 (2003) 125.
[5] Y. Idemoto, H. Sekine, K. Ui, N. Koura, Solid State Ionics 176 (2005) 299.
[6] S.-T. Myung, S. Komaba, N. Kumagai, H. Yashiro, H.-T. Chung, T.-H. Cho, Electrochim. Acta 47 (2002) 2543.
[7] Y.S. Lee, Y.K. Sun, S. Ota, T. Miyashita, M. Yoshino, Electrochem. Commun. 4 (2002) 989.
[8] S.H. Park, S.W. Oh, S.T. Myung, Y.K. Sun, Electrochem, Solid State Lett. 7 (2004) A451.
[9] T.-F. Yi, X.-G. Hu, J. Power Sources 167 (2007) 185.
[10] N.M. Hagh, G.G. Amatucci, J. Power Sources 195 (2010) 5005.
[11] J.Y. Shi, C.-W. Yi, K. Kim, J. Power Sources 195 (2010) 6860.
[12] Y. Idemoto, N. Kitamura, H. Iwatsuki, Electrochemistry 76 (2008) 808.
[13] N. Kitamura, H. Iwatsuki, Y. Idemoto, J. Power Sources 189 (2009) 114.
[14] F. Izumi, T. Ikeda, Mater. Sci. Forum 198 (2000) 321.
[15] F. Izumi, J. Crystallogr. Soc. Jpn. 44 (2002) 380.